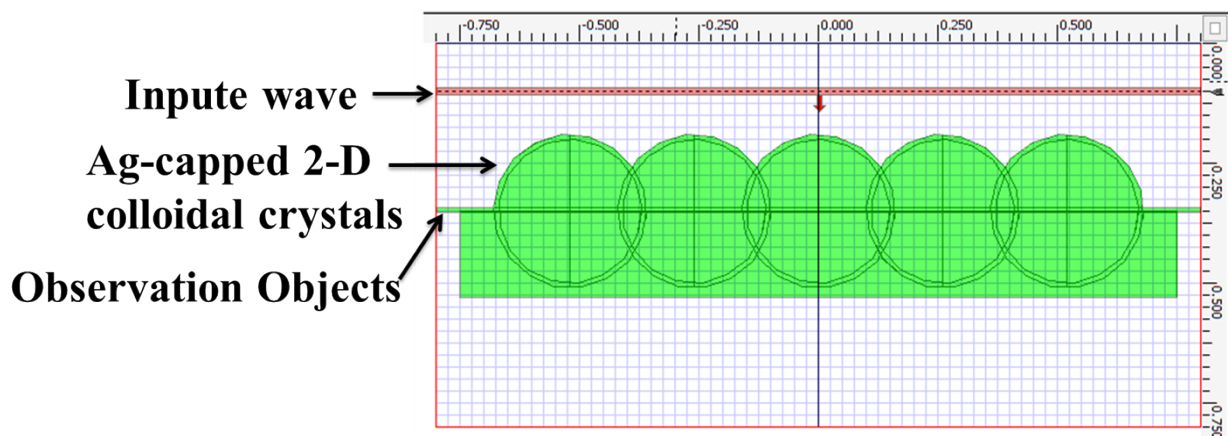


## Supporting Information for

### Control of Plasmonic Fluorescence Enhancement on Self-Assembled 2-D Colloidal Crystals

5 By *Wei Hong*,<sup>†</sup> *Yu Zhang*,<sup>†</sup> *Lin Gan*, *Xudong Chen*\* and *Mingqiu Zhang*\*

10



**Figure S1.** Illustration showing the cross section of the FDTD model of the Ag-capped 2-D colloidal crystals. Firstly, Ag semispheres or Ag@PVA semispheres were formed by removing the lower half of the spheres by air. After that the PS spheres with smaller radius were added to remove the Ag core to have the Ag-capped 2-D colloidal crystals structures.

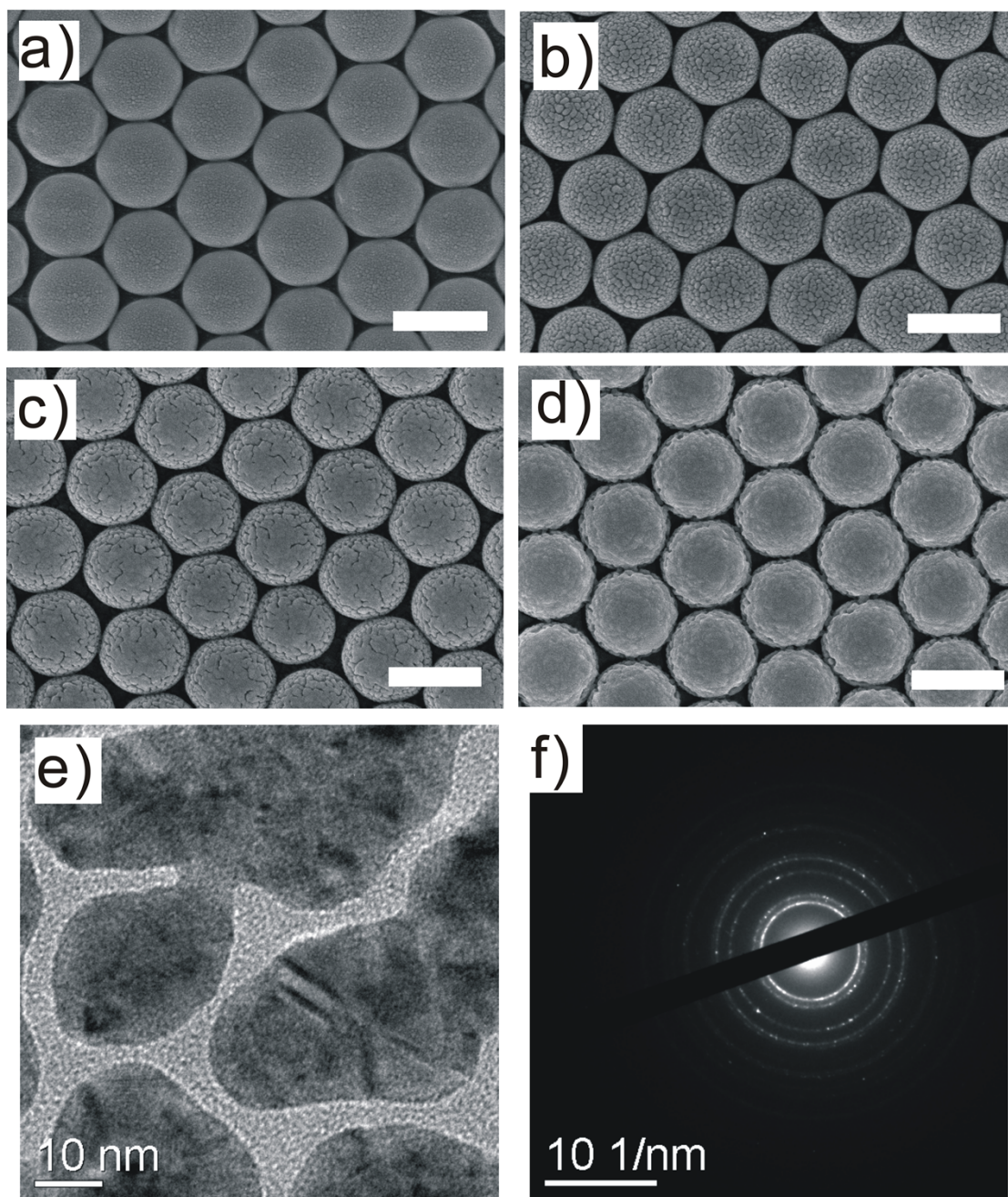


**Figure S2.** SEM images of PS400/Ag samples with different thickness of Ag cap: (a) 2.5 nm; (b) 5 nm; (c) 10 nm; (d) 20 nm. Scale bar: 400 nm. TEM images (e) and electron diffraction (f) of PS400/Ag 5 samples with thickness of 10 nm. As the silver films in this work were prepared via sputtering deposition, the Ag grains were nanocrystals as evidenced by the electron diffraction rings of polycrystals. However, the precise grain sizes were difficult to measure because few lattice fringes could be observed under high resolution TEM.

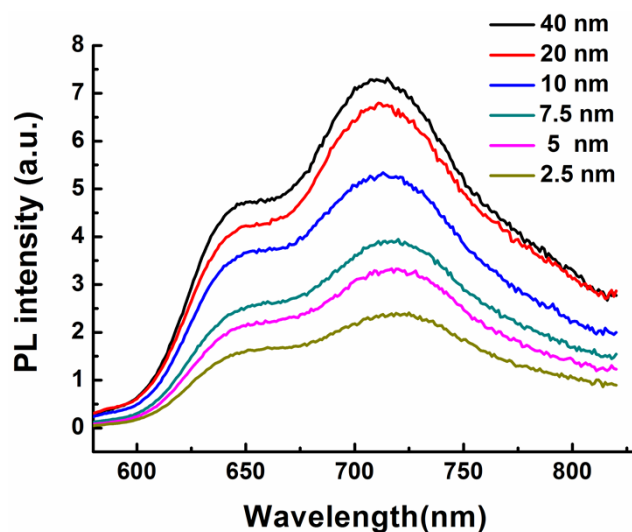


**Figure S3.** Fluorescence spectra of P3HT layer on PS400/Ag substrates with different Ag cap thickness ( $\lambda_{\text{ex}}=555$  nm).

5

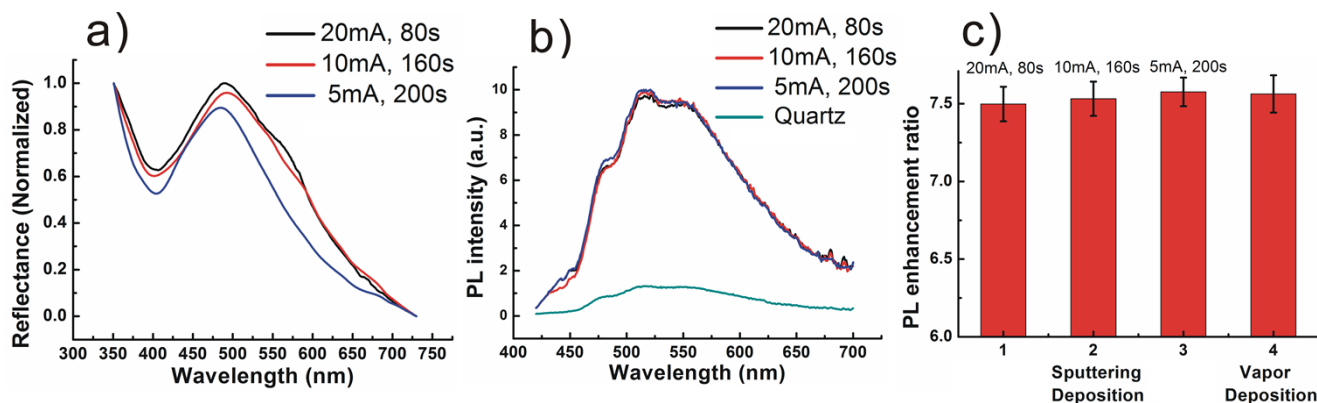


**Figure S4.** Comparison between the reflectance spectra (a) and fluorescence spectra of PCFOz on PS300/Ag samples with silver thickness of 20 nm by different sputtering current. (c) Comparison between the enhancement ratios for PCFOz on PS300/Ag samples with thickness of 20 nm by 10 sputtering deposition and vapor deposition. As the results showed, no significant differences were observed between three sputtering deposition samples as well as the vapor deposition sample, indicating that the Ag grain size might not influence significantly to the plasmonic fluorescence enhancement.

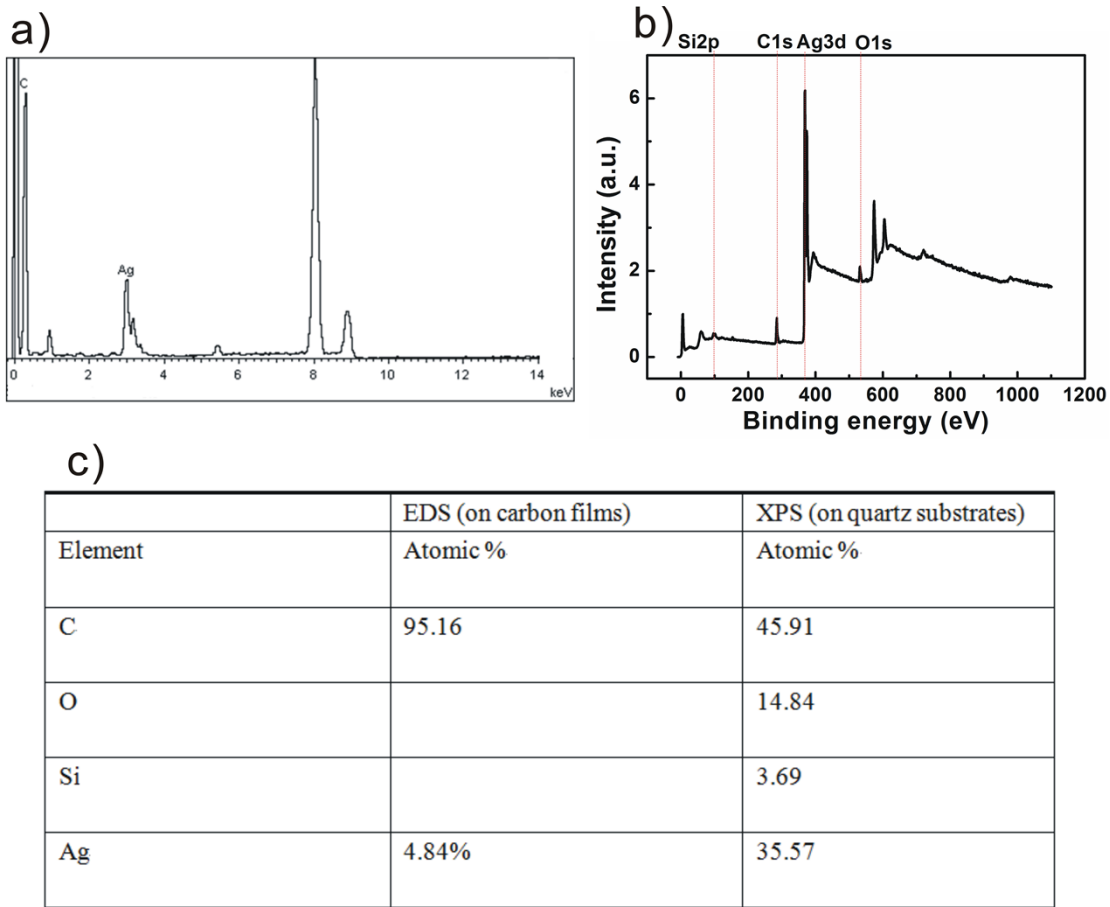


**Figure S5.** Elemental analysis on the PS300/Ag samples with silver thickness of 20 nm by (a) EDS (by JEOL JEM-2010H, on carbon films, two days in the air after the preparation) and (b) XPS (by 5 ESCALAB 250, Thermofisher Scientific, equipped with a monochromatic X-ray source, Al K $\alpha$ , 1486.6 eV, on quartz substrates, two days in the air after the preparation).

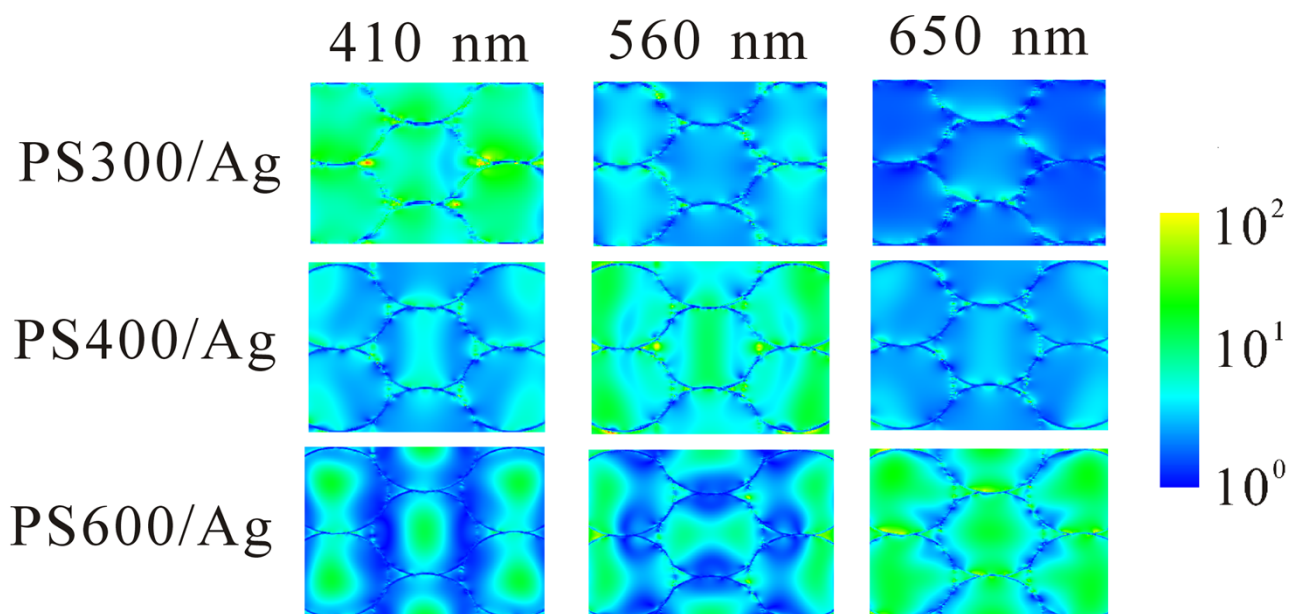
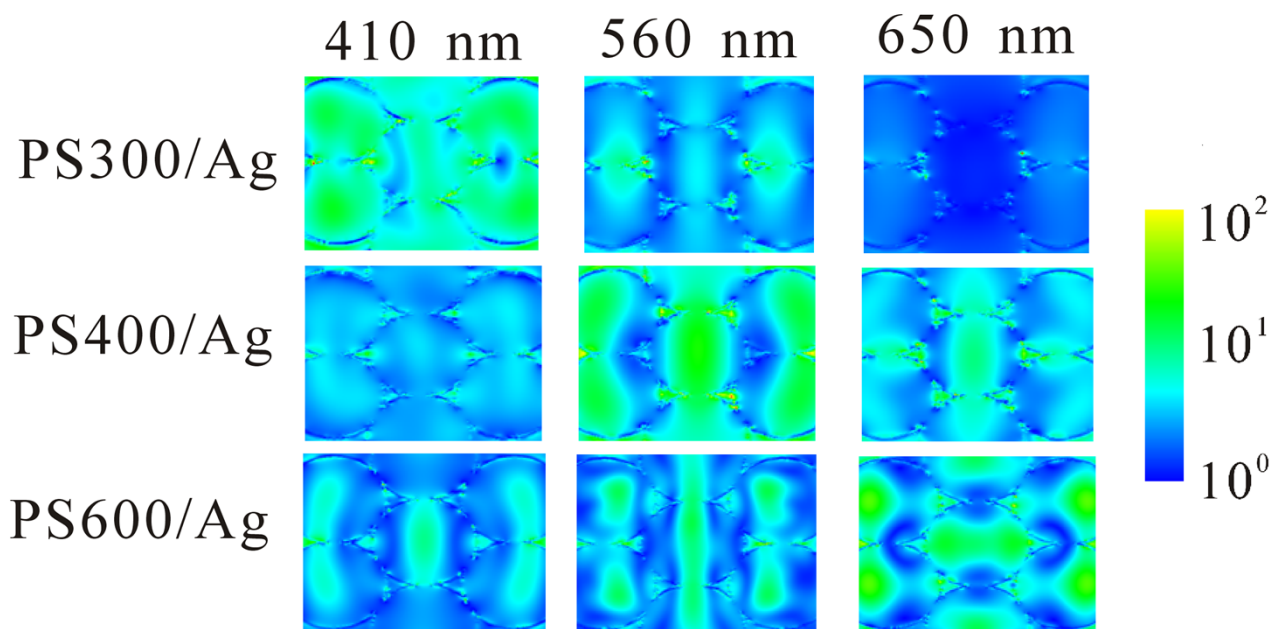


**Figure S6.** Comparison between relative electric field enhancement around the PS300/Ag, PS400/Ag and PS600/Ag samples in air at 410 nm, 560 nm and 650 nm excitation wavelength, respectively.



5 **Figure S7.** Comparison between relative electric field enhancement around the PS300/Ag, PS400/Ag and PS600/Ag samples covered with 10 nm PVA films at 410 nm, 560 nm and 650 nm excitation wavelength, respectively.

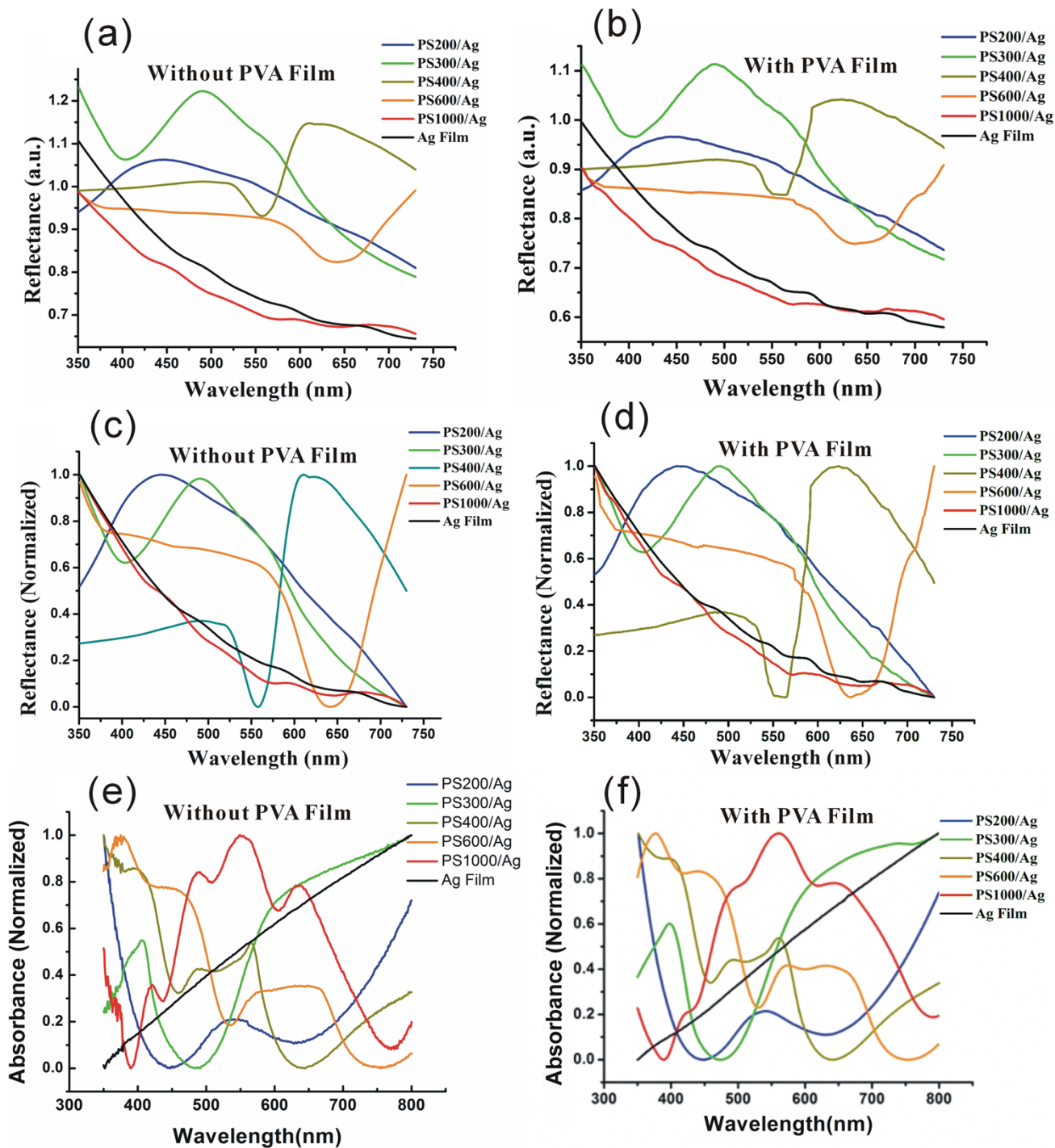


**Figure S8.** Comparison between the reflectance spectra (a,b), normalized reflectance spectra (c,d) and normalized extinction spectra (e,f) of the Ag film, PS200/Ag, PS300/Ag, PS400/Ag, PS600/Ag and PS1000/Ag samples with and without 10 nm PVA coatings, respectively.

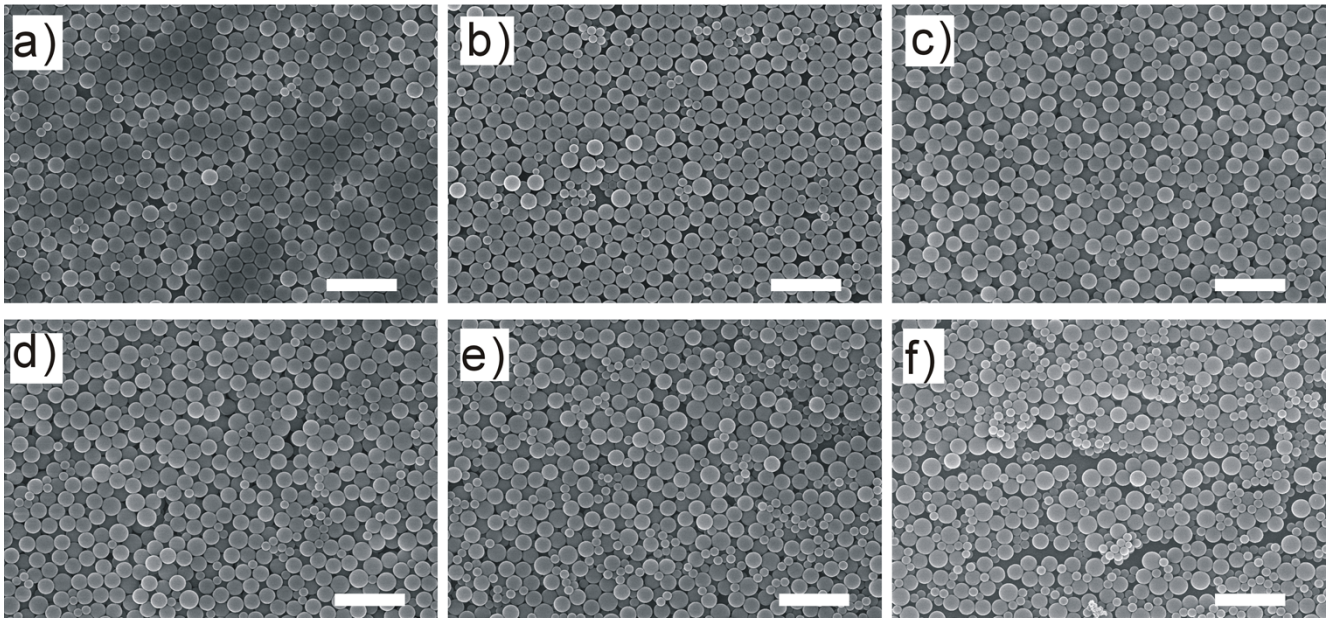


**Figure S9.** SEM images of disordered PS400/Ag samples obtained over a range of volume compositions 200 nm: 400 nm: 600 nm=x:1-x:x PS spheres suspension, in which x was: (a) 0.05; (b) 0.1; (c) 0.15; (d) 0.20; (e) 0.25; (f) 0.30. Scale bar: 2000 nm.

5

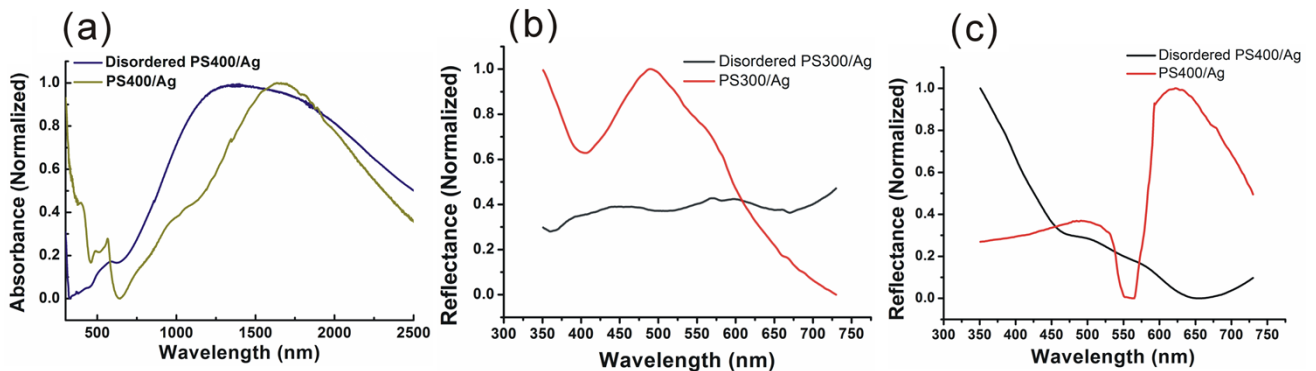


**Figure S10.** (a) Normalized extinction spectra and (c) normalized reflectance spectra for ordered and disordered 20-nm-thick Ag-capped PS 2-D colloidal crystals with sphere average diameters of 400 nm on quartz substrates. (b) Normalized reflectance spectra for ordered and disordered 20-nm-thick Ag-capped PS 2-D colloidal crystals with sphere average diameters of 300 nm on quartz substrates. The disordered PS400/Ag sample was prepared by mixing 200 nm, 400 nm and 600 nm PS sphere suspension by 3:4:3 volume ratio. The disordered PS300/Ag sample was prepared by mixing 200 nm, 300 nm and 400 nm PS sphere suspension by 3:4:3 volume ratio.

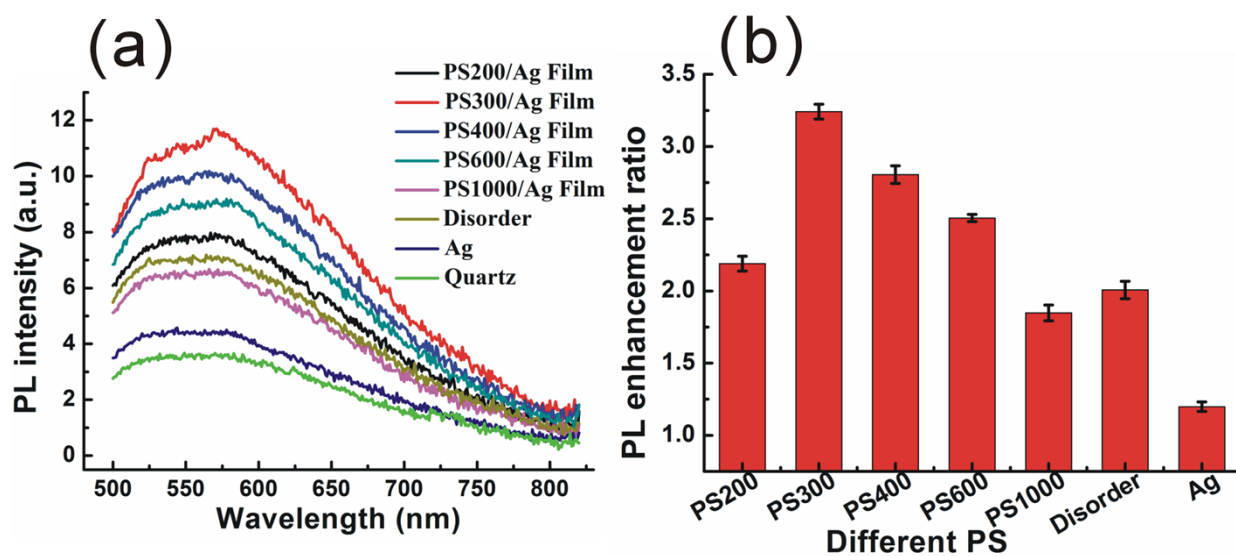


**Figure S11.** (a) Fluorescence spectra of acriflavine layer on different substrates ( $\lambda_{ex}=455$  nm). (b) The enhancement ratio of acriflavine layer on different substrates at  $\lambda_{em}=560$  nm.

5

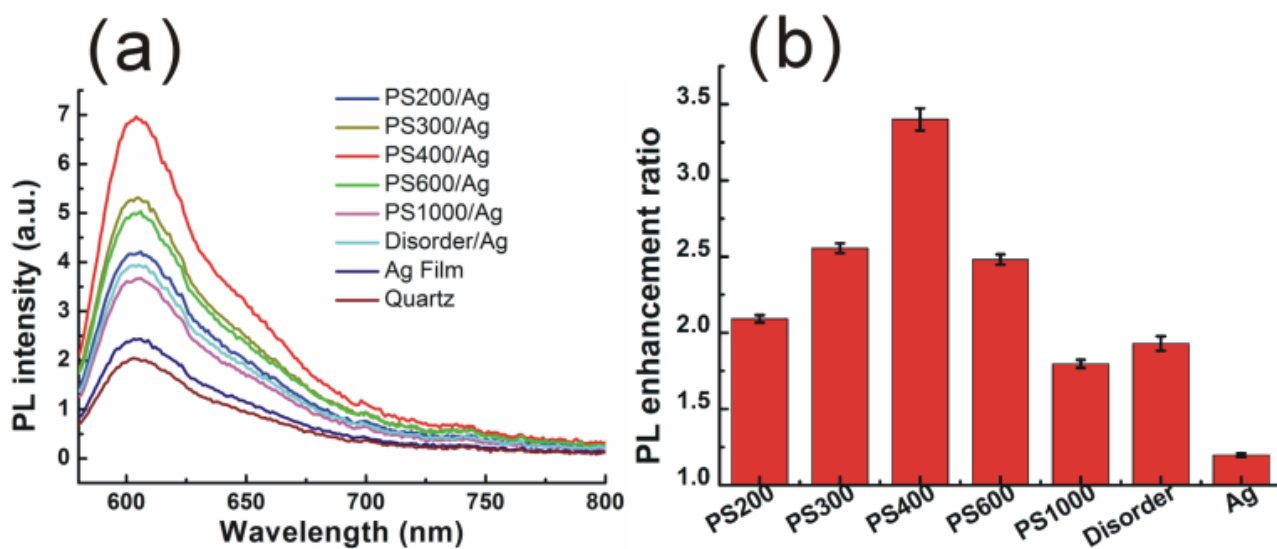


**Figure S12.** (a) Fluorescence spectra of rhodamine B layer on different substrates ( $\lambda_{ex}=565$  nm). (b) The enhancement ratio of rhodamine B layer on different substrates at  $\lambda_{em}=610$  nm.



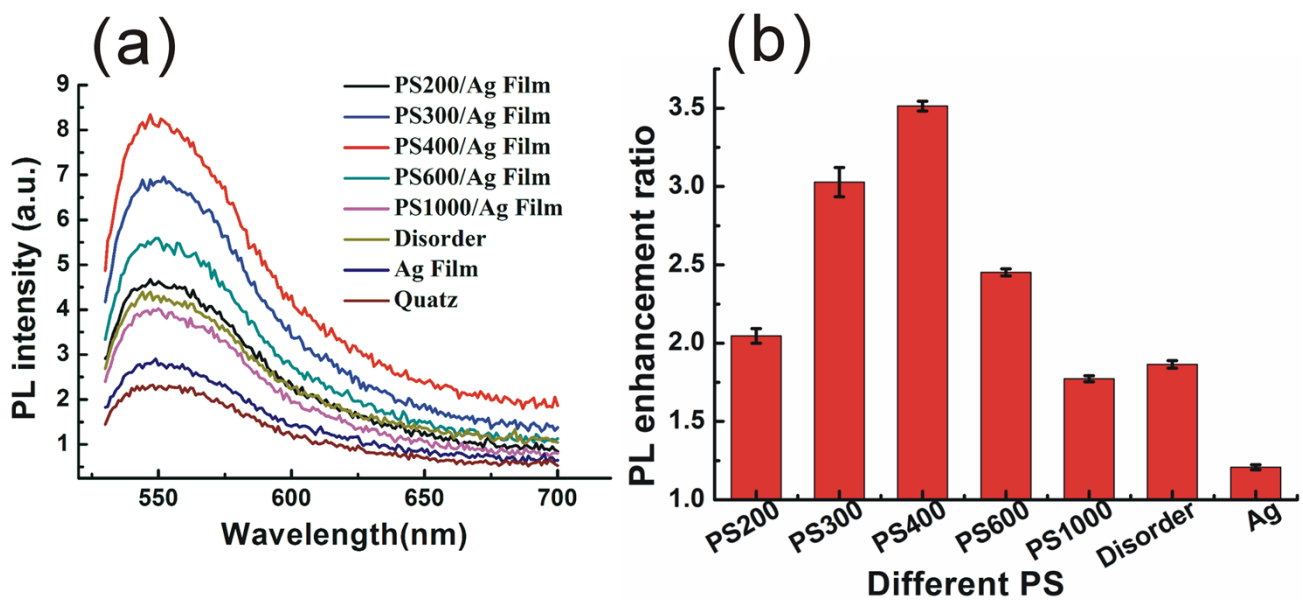


**Figure S13.** (a) Fluorescence spectra of fluorescein sodium layer on different substrates ( $\lambda_{ex}=507$  nm). (b) The enhancement ratio of fluorescein sodium layer on different substrates at  $\lambda_{em}=550$  nm.

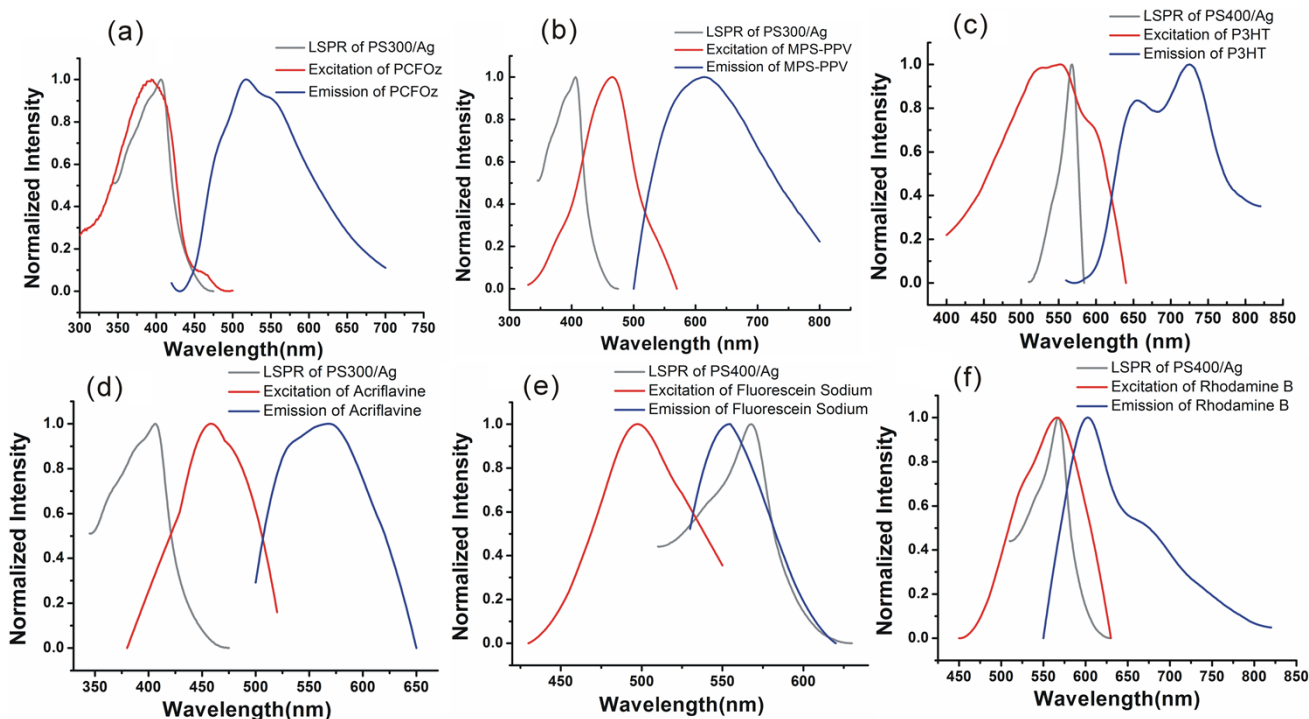


**Figure S14.** Normalized excitation and emission spectra (red and blue line traces, respectively) of the fluorophore layers overlapping with corresponding LSPRs (gray traces) of the substrates: (a) PCFOz layer with LSPR of PS300/Ag; (b) MPS-PPV layer with LSPR of PS300/Ag; (c) P3HT layer with LSPR of PS400/Ag; (d) acriflavine layer with LSPR of PS300/Ag; (e) fluorescein sodium layer with LSPR of PS400/Ag; (f) rhodamine B layer with LSPR of PS400/Ag, respectively. As shown in the figure, the excitation maxima of PCFOz, MPS-PPV and acriflavine overlaps with LSPR of PS300/Ag effectively, corresponding to their fluorescence enhancement ratio in Fig4, Fig.5 and Fig.S9, respectively; the excitation maxima of P3HT, fluorescein sodium and rhodamine B overlaps with LSPR 10 of PS400/Ag effectively, corresponding to their fluorescence enhancement ratio in Fig6, Fig.S11 and Fig.S10, respectively.

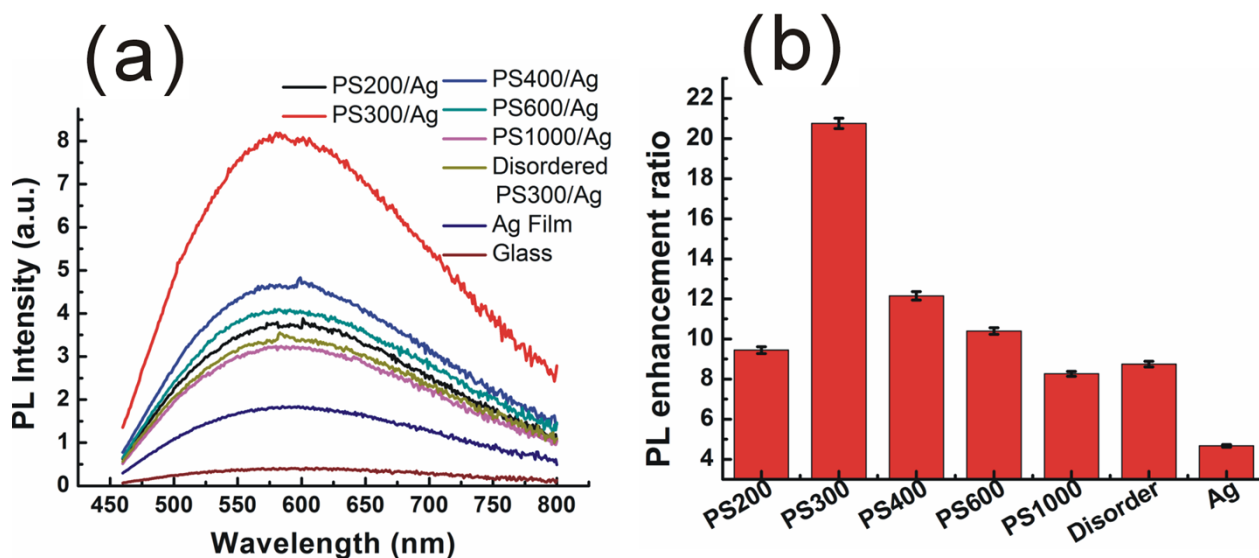


**Figure S15.** (a) Fluorescence spectra of conjugated polymer MPS-PPV layer on different substrates ( $\lambda_{ex}=405$  nm). (b) The enhancement ratio of different substrates at  $\lambda_{em}=600$  nm.

5

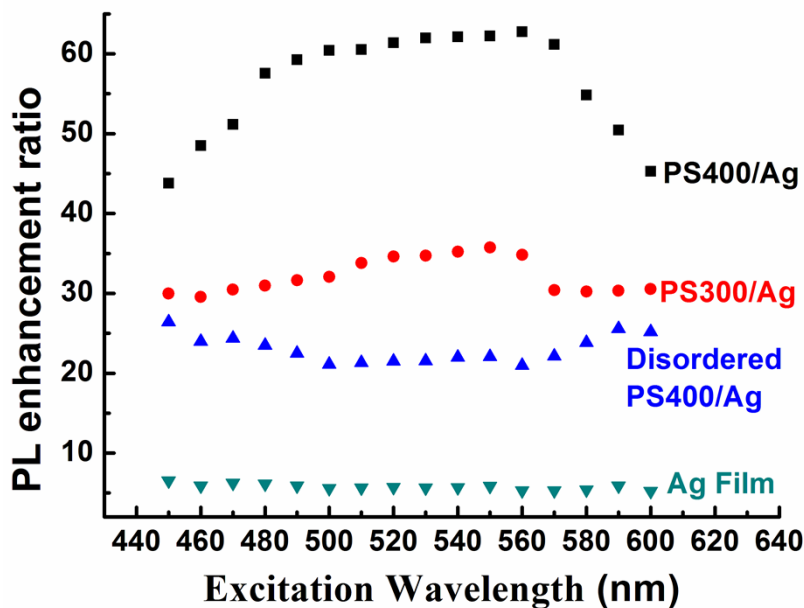


**Figure S16.** Plots of the excitation wavelength for P3HT layer versus the PL enhancement ratio for Ag film, PS300/Ag, PS400/Ag and disordered PS400/Ag.

10

**Table S1** The measured values of lifetime ( $\tau$ , ps), the goodness of the fit parameter ( $\chi_{R2}$ ), the quantum yield ratios ( $Q_m$ ), and the values of the excitation enhancement and emission enhancement for each Ag-capped sample of MPS-PPV versus a quartz surface ( $Q_0=0.1$ ).

Sample	$\tau$	$\chi_{R2}^2$	$Q_m$	$E_{em} = Q_m/Q_0$	$E_f$	$E_{ex}$
Quartz	551	1.26				
Ag-film	366	1.46	0.402	4.012	4.69	1.167
PS200/Ag	251	1.12	0.590	5.902	9.45	1.602
PS300/Ag	121	1.48	0.802	8.017	20.69	2.581
PS400/Ag	180	1.42	0.706	7.063	12.13	1.718
PS600/Ag	30	1.40	0.625	6.251	10.32	1.652
PS1000/Ag	268	1.10	0.562	5.622	8.278	1.472
Disordered PS300/Ag	260	1.11	0.575	5.753	8.782	1.527

5

**Table S2** The measured values of lifetime ( $\tau$ , ps), the goodness of the fit parameter ( $\chi_{R2}$ ), the quantum yield ratios ( $Q_m$ ), and the values of the excitation enhancement and emission enhancement for each 10 Ag-capped sample of acriflavine versus a quartz surface ( $Q_0=0.8$ ).

Sample	$\tau$	$\chi_{R2}^2$	$Q_m$	$E_{em} = Q_m/Q_0$	$E_f$	$E_{ex}$
Quartz	2919	1.78				
Ag-film	1979	1.63	0.932	0.864	1.198	1.386
PS200/Ag	442	1.16	0.985	0.970	2.189	2.258
PS300/Ag	140	1.16	0.995	0.990	3.241	3.273
PS400/Ag	198	1.06	0.993	0.986	2.805	2.844
PS600/Ag	366	1.08	0.987	0.975	2.505	2.569
PS1000/Ag	493	1.21	0.983	0.966	1.847	1.912
Disordered PS300/Ag	471	1.02	0.984	0.968	2.007	2.074